IRESPUB Journal of Environmental & Material Sciences
ISSN: 2770-4084
Volume: 4 | Issue: 1 | JAN – FEB 2025 | Available Online: www.irespub.com
https://doi.org/10.62179/irespub-jems.v4i1.1

# Radiogenic Heat Production in Selected River Sediments of Bungoma County, Kenya

**Michael Nakitare Waswa & Mukanda Kere Wanyama**

Department of Science, Technology & Engineering; Kibabii University, 1699-50200 Bungoma

**ABSTRACT**

This study is aimed at investigating the radiogenic heat production in the sediment samples using measurements of primordial radionuclide concentrations of uranium, thorium, and potassium in the major rivers of Bungoma County, Kenya. A gamma-ray spectrometer is used to obtain varied data on naturally occurring radionuclides in the samples from the ten rivers and reveals the contents and the distribution of the radioactive elements. The results show that the contribution and rate of heat production of 40-K, 238-U, and 232-Th in the samples vary significantly with geological locations, with 232Th and 40K as the major elements that predominate in heat production in the study area, with 238U also contributing significantly. The mean heat produced by uranium, thorium, and potassium is $321.0223\times10^{-5}$ρwkg$^{-1}$, $7772.659\times10^{-5}$ρwkg$^{-1}$ and $7196.131\times10^{-5}$ρwkg$^{-1}$respectively. The total heat produced in the study area varied from $9.191292\times10^{-5}$ρwkg$^{-1}$ to $63408.01\times10^{-5}$ρwkg$^{-1}$, which can classify the study area as Low-to-Moderate Heat Production Potential zone.

**KEYWORDS**

radiogenic heat production; primordial radionuclides; gamma-ray spectrometry.

## 1 INTRODUCTION

The decay of long-lived radioactive isotopes is one of the sources of the Earth's internal heat. This radioactive decay is the major source of the Earth's interior heat, which in turn, powers all geodynamic processes [1]. During radioactive decay, mass is changed into energy. Except for the tiny amount associated with the antineutrino and neutrinos generated in β- and β+ decay or electron capture, respectively, all of the energy ends up as heat. During the decay process of the radioactive nuclides in rocks, the emission of α, β, γ particles changes into radiogenic heat [2]. The amount of radiogenic heat per unit time (i.e. rate of radiogenic heat production) generated from rocks is independent of occurrence forms, temperature, and pressure of the rocks, but determined only by the concentration of the radioactive nuclides in the rocks [3]. The decay of 238U and 232Th are the main heat producers today with heat production constants of 9.52 x 10-5w kg-1 and 2.56 x 10-5w kg-1, respectively [4]. The least heat producer is 40K compared to 238U, and 232Th with a heat production constant of 3.48 x 10-9w kg-1[5]. The heat produced in the mantle and crust of the Earth during the decay of 238U, 232Th, and 40K is referred to as Radiogenic Heat Production or RHP [6]. Certain peaks in the corresponding γ-spectra are characteristic for the different decay series while the continuous background spectrum is due to Compton-scattering and photoelectric absorption.

River sediments are regarded to be the host of environmental waste discharge by natural and anthropogenic processes in our surroundings [7] and hence pile and transfer contaminants of varying degrees to a given geographical region. Most river sediments are formed when the rock and organic materials are broken into small pieces by fluvial means which enhances the levels of natural radioactivity in river sediments [8, 9]. The sediments' lithological and geochemical features influence the RHP values as reported by [10].

The assessment of the number of radioactive elements has been the subject of several studies during the last few decades, due to its importance in the thermal evaluation of the lithosphere. The primordial radioactive isotopes 232 Th, 40K, and 238U contribute most of the terrestrial heat flow.

These are fundamental in the understanding of the nature of the mantle, the heat-generating potential, and the crust of the earth. The energy emitted by all of these decay processes, consisting of the kinetic energy of the emitted particles and the γ-radiation associated with the different decay processes, is absorbed in the rocks and finally transformed into heat. The study of radiogenic heat production is thus important in shedding brightness on any anomalously high thermal regime in any region [1].

In this work, the well-calibrated Gamma-ray spectrometer was used to measure the concentration of radioactive elements such as Potassium (40K), Uranium (238U), and Thorium (232Th) in the river sediments of Bungoma County. The RHP determines the heat flow in the basement rocks from which river sediments are formed and has been used for the assessment of geothermal resources in many parts of the world and the interpretation of the continental heat flux data [11, 12]. The objective of this work is to investigate the radiogenic heat production potential and the patterns of heat production in the river sediments of the study area.

### 1.1 Physiography and Geological Setting of Bungoma County

Bungoma County is located in the Western part of Kenya, the former Western province. It is found on coordinates 00°34'00" N34'00" E. The area has an elevation of 4544 ft (1385 m). Geologically, Bungoma County is made of basement rocks which consist of schists, gneisses, and migmatites derived from the original sedimentary succession, which has been transformed by original metamorphism through crystallization of orogenic earth-movement into foliated quartz and feldspar-rich rocks with variable amounts of biotite and/or hornblende [13]. Around Mount Elgon region in the North where the basement system is seen before it last disappears, there is a volcanic series that further suggests that folding took place and gives evidence of repetition of quartzites and quartz-mica schists band [14]. The main rivers and streams in the region exhibit a radial drainage pattern from Mount Elgon. Most of these rivers are perennial types where the majority of them reach maturity on the Peneplains meandering in broad valleys but have rejuvenated and re-excavated their beds so that they now flow in gorges [15]. Kibisi, Kuywa, and Chwele are the main tributaries of river Nzoia. The geological map of Bungoma County which shows the river distribution in the area is presented in Figure 1.

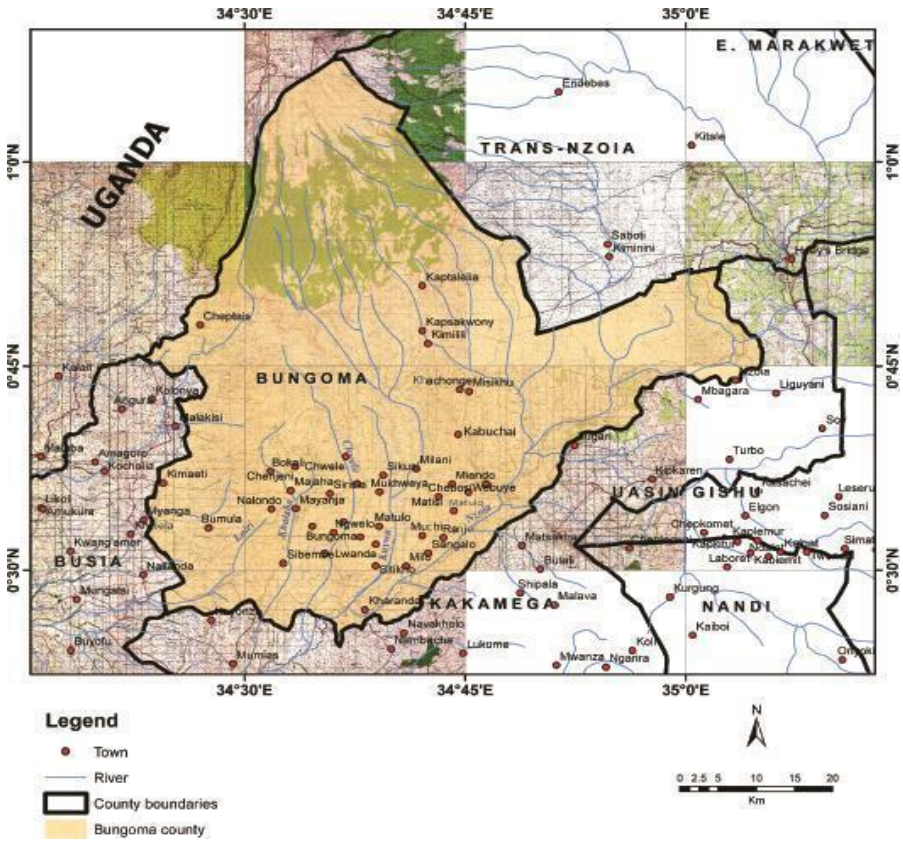


**FIGURE 1:** Map showing the study area.

### 1.2 Radiogenic Elements and Heat Production

The main isotopes that release heat are 238U, 235U, 232Th, and 40K. The isotope 235U has a shorter half-life than 238U and releases extra energy in its decay. The heat Q produced by radioactivity in a rock that has activity concentrations $C_U$, $C_{Th}$, and $C_K$ respectively, of these elements is given by equation 1[16, 17];

$$RHP(\mu w/m^3) = 10^{-5}\rho[9.52C_U(ppm) + 2.56C_{Th}(ppm) + 3.48C_K(\%)] \quad (1)$$

Conduction, convection, and radiation are the processes through which heat is transported. Conduction is the most important process of heat transport in solid materials. However, it is an inefficient type of heat transport and when the molecules are free to move, as in fluid or gas, the process of convection becomes more important. Although the mantle is solid from the standpoint of the rapid passage of seismic waves, the temperature is high enough for the mantle to act as a viscous fluid over long time intervals. Consequently, convection is also the most important form of heat transport in the fluid core [1].

## 2 MATERIALS AND METHOD OF MEASUREMENT

### 2.1. Sample Collection

A total of twenty (20) river sediment samples were collected from the ten (10) rivers spread around Bungoma County. The collected samples were labeled at the point of collection and the coordinates were recorded. The collected samples were put in the polythene bag and then transported to the laboratory for further processing. The selected river sites and their locations are listed in Table 1.

### 2.2. Sample Preparation

Samples obtained were put in plastic containers and labeling was done depending on the position from which the sample was taken. Samples were dehydrated in a hot sun or in an oven at a temperature of about 105°C to remove any moisture. Uniformity of the sizes of the grains was attained by the use of a sieve of diameter 2 mm so that the particles obtained are not greater than 2 mm in terms of diameter. Packing of the samples was done in standard 500 ml containers which were tightly closed to avoid any leakages, referenced, and labeled for comparison purposes. Secular equilibrium was achieved by keeping the samples for about thirty days to ensure that the rate of disintegration between $^{40}K$, $^{238}U$, $^{232}Th$, and their daughter nuclides is the same at any given time interval. After the secular equilibrium was attained, the gamma spectrometry measurement of the samples was then carried out using a well-calibrated NaI(Tl). The activity concentration of the radionuclides in every sample was determined by the use of a Gamma Ray Spectrometer for a period of around 5000 minutes to increase the precision of radioactive measurements [18].

## 3 ANALYSIS

The photopeak area values were converted into concentration in $Bqkg^{-1}$ and then later to part per million (ppm) (part per million), and presented in Table 2. These concentrations in ppm were later used for the determination of the radiogenic heat production using the Rybach equation (Eq. 1) where $C_U$, $C_{Th}$, and $C_K$ are concentrations in ppm of Uranium, Thorium, and Potassium, respectively. The total radiogenic heat production for each sample was obtained by summation of the three isotopes of heat production. The area under photo-peak represents the counts due to each radioactive nucleus and was computed from the memory of the Multichannel Analyzer (M.C.A.).

## 4 RESULTS AND DISCUSSION

Considering the distribution of the radiogenic heat production elements (RHPE) contribution, it can be seen from the pattern of the distribution shown in Table 2 and Figure 2, that Th and K are the major elements that predominates in heat production. The contribution by U is low but significant.

**TABLE 1:** Radionuclide Activity concentration of the sediment samples.

| Sample Code | $^{238}U$ (Bq/Kg) | $^{232}Th$ (Bq/Kg) | $^{40}K$ (Bq/Kg) | $^{238}U$ (ppm) | $^{232}Th$ (ppm) | $^{40}K$ (ppm) |
|---|---|---|---|---|---|---|
| S1 | 1.08 | 52.62 | 571.21 | 13.5 | 213.6372 | 1787.887 |
| S2 | 1.05 | 168.05 | 1.08 | 13.125 | 682.283 | 3.3804 |
| S3 | 1.09 | 1.05 | 54.62 | 13.625 | 4.263 | 170.9606 |
| S4 | 1.09 | 57.77 | 168.05 | 13.625 | 234.5462 | 525.9965 |
| S5 | 2.11 | 310.8 | 1.05 | 26.375 | 1261.848 | 3.2865 |
| S6 | 0.03 | 1.09 | 57.77 | 0.375 | 4.4254 | 180.8201 |
| S7 | 2.11 | 33.60 | 310.8 | 26.375 | 136.416 | 972.804 |
| S8 | 2.14 | 454.66 | 1.09 | 26.75 | 1845.92 | 3.4117 |
| S9 | 1.08 | 1.09 | 33.60 | 13.5 | 4.4254 | 105.168 |
| S10 | 2.13 | 51.48 | 454.66 | 26.625 | 209.0088 | 1423.086 |
| S11 | 2.11 | 433.68 | 1.09 | 26.375 | 1760.741 | 3.4117 |
| S12 | 1.05 | 2.11 | 51.48 | 13.125 | 8.5666 | 161.1324 |
| S13 | 2.14 | 51.48 | 433.68 | 26.75 | 209.0088 | 1357.418 |
| S14 | 3.18 | 174.32 | 2.11 | 39.75 | 707.7392 | 6.6043 |
| S15 | 1.07 | 0.03 | 51.48 | 13.375 | 0.1218 | 161.1324 |
| S16 | 1.08 | 33.60 | 174.32 | 13.5 | 136.416 | 545.6216 |
| S17 | 1.05 | 550.29 | 0.03 | 13.125 | 2234.177 | 0.0939 |
| S18 | 2.10 | 2.11 | 33.60 | 26.25 | 8.5666 | 105.168 |
| S19 | 4.24 | 78.79 | 551.29 | 53 | 319.8874 | 1725.538 |
| S20 | 1.08 | 2.11 | 2.11 | 13.5 | 8.5666 | 6.6043 |
| **AV** | **1.65** | **123.04** | **147.76** | | | |
| **MAX** | **4.24** | **550.29** | **571.21** | | | |
| **MIN** | **0.03** | **0.03** | **0.03** | | | |

**TABLE 2:** Potential Radiogenic Heat.

| Sample code | U-238 (ppm) | Th-232 (ppm) | K-40 (ppm) | RHP-U $\times 10^{-5}$ Pwkg$^{-1}$ | RHP-Th $\times 10^{-5}$ Pwkg$^{-1}$ | RHP-K $\times 10^{-5}$ Pwkg$^{-1}$ | Total Heat Q $\times 10^{-5}$ Pwkg$^{-1}$ |
|---|---|---|---|---|---|---|---|
| S1 | 13.5 | 213.6372 | 1787.887 | 210.06 | 3324.195 | 27819.53 | 31353.78 |
| S2 | 13.125 | 682.283 | 3.3804 | 204.225 | 10616.32 | 52.59902 | 10873.14 |
| S3 | 13.625 | 4.263 | 170.9606 | 212.005 | 66.33228 | 2660.147 | 2938.484 |
| S4 | 13.625 | 234.5462 | 525.9965 | 212.005 | 3649.539 | 8184.506 | 12046.05 |
| S5 | 26.375 | 1261.848 | 3.2865 | 410.395 | 19634.35 | 51.13794 | 20095.88 |
| 56 | 0.375 | 4.4254 | 180.8201 | 5.835 | 68.85922 | 2813.561 | 2888.255 |
| S7 | 26.375 | 136.416 | 972.804 | 410.395 | 2122.633 | 15136.83 | 17669.86 |
| S8 | 26.75 | 1845.92 | 3.4117 | 416.23 | 28722.51 | 53.08605 | 29191.83 |
| S9 | 13.5 | 4.4254 | 105.168 | 210.06 | 68.85922 | 1636.414 | 1915.333 |
| S10 | 26.625 | 209.0088 | 1423.086 | 414.285 | 3252.177 | 22143.22 | 25809.68 |
| S11 | 26.375 | 1760.741 | 3.4117 | 410.395 | 27397.13 | 53.08605 | 27860.61 |
| S12 | 13.125 | 8.5666 | 161.1324 | 204.225 | 133.2963 | 2507.22 | 2844.741 |
| S13 | 26.75 | 209.0088 | 1357.418 | 416.23 | 3252.177 | 21121.43 | 24789.84 |
| S14 | 39.75 | 707.7392 | 6.6043 | 618.51 | 11012.42 | 102.7629 | 11733.69 |
| S15 | 13.375 | 0.1218 | 161.1324 | 208.115 | 1.895208 | 2507.22 | 2717.23 |
| S16 | 13.5 | 136.416 | 545.6216 | 210.06 | 2122.633 | 8489.872 | 10822.57 |
| S17 | 13.125 | 2234.177 | 0.0939 | 204.225 | 34763.8 | 1.461084 | 34969.49 |
| S18 | 26.25 | 8.5666 | 105.168 | 408.45 | 133.2963 | 1636.414 | 2178.16 |
| S19 | 53 | 319.8874 | 1725.538 | 824.68 | 4977.448 | 26849.37 | 32651.49 |
| S20 | 13.5 | 8.5666 | 6.6043 | 210.06 | 133.2963 | 102.7629 | 446.1192 |
| **AV** | **20.63125** | **499.5282** | **462.4763** | **321.0223** | **7772.659** | **7196.131** | **15289.81** |
| **MAX** | **53** | **2234.177** | **1787.887** | **824.68** | **34763.8** | **27819.53** | **63408.01** |
| **MIN** | **0.375** | **0.1218** | **0.0939** | **5.835** | **1.895208** | **1.461084** | **9.191292** |

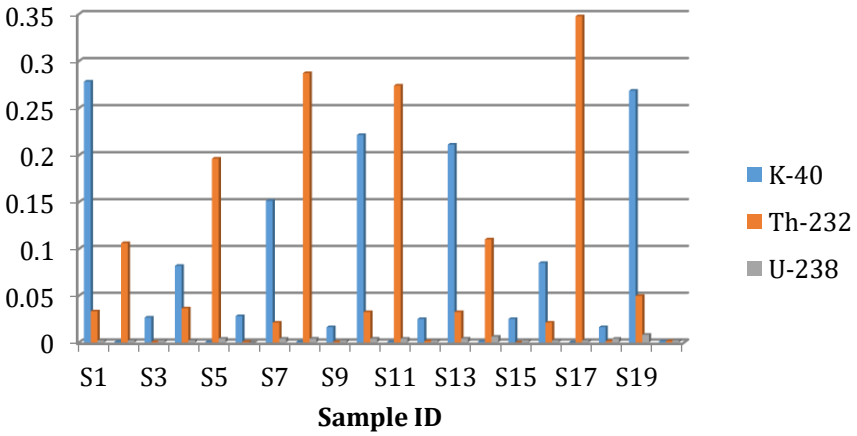


**FIGURE 2:** Trends of radiogenic heat production in the study area.

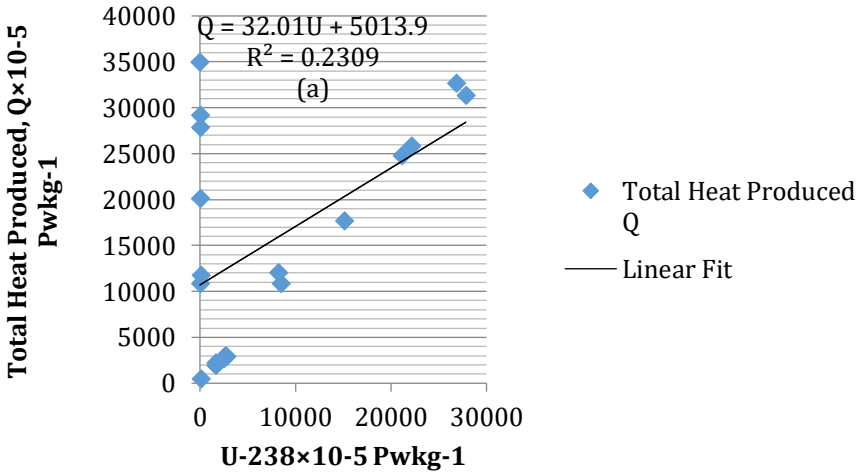


**FIGURE 3A:** Contribution to the total RHP by U-238.

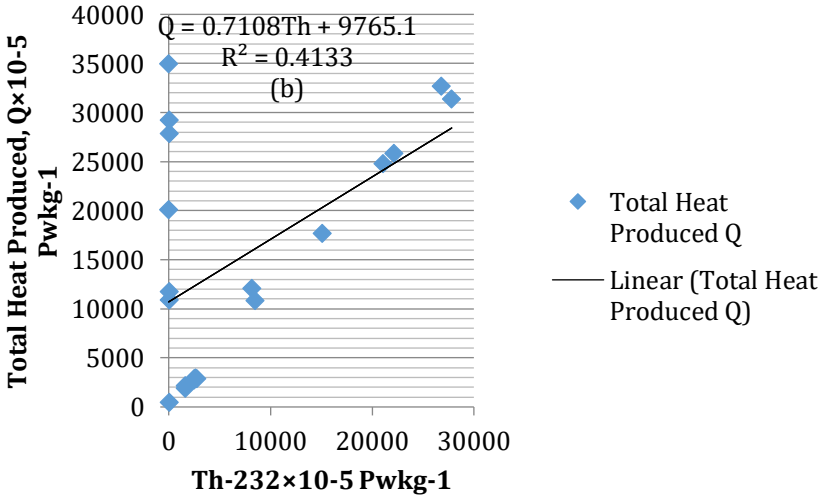


**FIGURE 3B:** Contribution to the total RHP by Th-232.

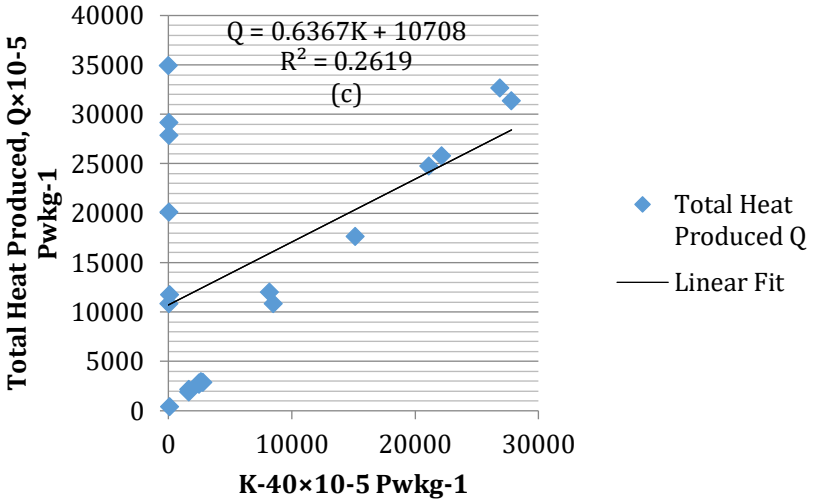


**FIGURE 3C:** Contribution to the total RHP by K-40.

The linear relations between the radionuclides and the total heat produced in the study area are shown in Figure 2. The linear models and the correlation coefficients (R) between Q and uranium, thorium, and potassium are: Q= 32.01U+5013.19, with R= 0.2309 for 238U; Q= 0.7108Th+9765.1, with R=0.4133 for 232Th; and Q= 0.6367K+10708, with R=0.2619 for 40K respectively. The relations exhibit strong correlation coefficients. In Fig. 3a between 238U and total heat produced; in Figure 3b between 232Th and total heat produced, and in Figure 3c between 40-K and total heat produced respectively. This implies, that the higher the uranium thorium and potassium, the higher the total heat produced in the study area. From Figure 2, it can be underscored that the contributions by the three radionuclides could be from the same source. The differences in radiogenic heat produced could be due to differences like the parent rocks underlying the revers and consequently their weathering effects. The models (Fig.2) reveal that no matter how small the geogenic contribution might be from any of these three basic radionuclides, they are of importance in the production of total radiogenic heat in the river sediments of Bungoma County, Kenya.

## CONCLUSION

From the findings, it is observed that there is irregular contribution of the studied radionuclides (U, Th, and K) to the radiogenic heat production in the river sediments as a result of their difference in geological locations where samples were taken from. Hence the model of radiogenic heat production of river sediments of Bungoma County has Th and K as the major elements, which predominate in heat production while the contribution of U may be considered fair.

## REFERENCES

[1] Ojo, E. O., Shittu, H. O., Adelowo, A. A., Ossai, B. N., & Amemfiene, C. B. (2015). The Model of Radiogenic Heat Production in the Federal Capital Territory (FCT), Abuja, Nigeria. International Journal of Modern Physics and Applications, 1(5), 200-204.

[2] Akin, U., & Ciftçi, Y. (2023). Heat flow of the kirşehir massif and geological sources of the radiogenic heat production. Bulletin of the Mineral Research and Exploration, 2011(143).

[3] Zhang, B., Wu, J., Ling, H., & Chen, P. (2007). Estimate of influence of U-Th-K radiogenic heat on cooling process of granitic melt and its geological implications. Science in China Series D: Earth Sciences, 50(5), 672-677.

[4] Murugesan, S., & Ravichandran, S. (2023). Radioactive heat production rate and excess lifetime cancer risk of sand from two major rivers in India–A comparative study. International Journal of Radiation Research, 21(1), 117-124.

[5] Sathish, V., Chandrasekaran, A., Manigandan, S., Tamilarasi, A., & Thangam, V. (2022). Assessment of natural radiation hazards and function of heat production rate in lake sediments of Puliyanthangal Lake surrounding the Ranipet industrial area, Tamil Nadu. Journal of Radioanalytical and Nuclear Chemistry, 331(3), 1495-1505.

[6] Murugesan, S., Mullainathan, S., Ramasamy, V., & Meenakshisundaram, V. (2016). Environmental radioactivity, magnetic measurements and mineral analysis of major South Indian river sediments. J. Mater. Environ. Sci, 7(7), 2375-2388.

[7] El-Taher, A., & Abbady, A. G. (2012). Natural radioactivity levels and associated radiation hazards in Nile river sediments from Aswan to El-Minia, Upper Egypt.

[8] Bouhila, G., Benrachi, F., & Ramdhane, M. (2018). Levels and effects of natural radionuclides in sediment banks of Rhumel River (Northeast Algeria). Cumhuriyet Science Journal, 39(2), 349-356.

[9] Ononugbo, C. P., Avwiri, G. O., & Ogan, C. A. (2016). Natural radioactivity measurement and evaluation of radiological hazards in sediment of Imo River, in rivers state, Nigeria by gamma ray spectrometry. Journal of Applied Physics, 3(1), 75-83.

[10] Najam, L. A., Al-Dbag, S. T., Wais, T. Y., & Mansour, H. (2022). Radiogenic heat production from natural radionuclides in sediments of the Tigris river in Mosul City, Iraq. International Journal of Nuclear Energy Science and Technology, 15(3-4), 302-316.

[11] Asere, A. M., & Sedara, S. O. (2020). Determination of Natural Radioactivity Concentration and Radiogenic Heat Production in Selected Quarry Sites in Ondo State, Nigeria. Journal of Science and Technology Research, 2(3).

[12] Olanyaa, A., Okellob, D., Oruruc, B., & Kisolod, A. Natural Radioactivity Levels and Radiogenic Heat Production in River Sediments from Gulu and Amuru Districts, Northern Uganda.

[13] Grupen C. (1996). Particle detectors, Cambridge University Press. pp30-35.

[14] Schoeman, D. J & Hawke, F. (1948). The fruit-coat fat of myricacordifollia-cape berry wax. South African Journal of Chemistry, 1(1), 5-13.

[15] Ingana, T. Z. (1993). Remote sensing: Application to the geological mapping with reflectance implication of rocks of the Webuye-Bungoma area (Doctoral dissertation).

[16] Rybach, L. (1988). Determination of heat production rate. Handbook of terrestrial heat flow density determinations.

[17] Asfahani, J. (2019). Heat production estimation by using natural gamma-ray well-logging technique in phosphatic khneifis deposit in Syria. Applied Radiation and Isotopes, 145, 209-216.

[18] Tzortzis, M., Tsertos, H., Christofides, S., &Christoduolides, G. (2003). Gamma-ray measurements of naturally occurring radioactive samples from Cyprus characteristic geological rocks. Radiation measurements, 37(3), 221-229.